PROCEEDINGS

of the

1992 BATTLEFIELD ATMOSPHERICS CONFERENCE

1–3 December 1992

Sponsor

Battlefield Environment Directorate
U.S. Army Research Laboratory
White Sands Missile Range, New Mexico

Conference Manager

Mr. Robert Lee
U.S. Army Research Laboratory

Conference Chairman

Mr. Edward Creegan
U.S. Army Research Laboratory

Host

Fort Bliss, El Paso Texas

SESSION IV: ATMOSPHERIC EFFECTS

SESSION V: WEATHER DECISION AIDS

SESSION I POSTERS: ATMOSPHERIC MODELING

PROGRESS IN ATMOSPHERIC PROPAGATION MODELING

AT FREQUENCIES BELOW 1000 GHz

H. J. Liebe, G. A. Hufford, and M. G. Cotton
National Telecommunications and Information Administration
Institute for Telecommunication Sciences, ITS.S3
Boulder, CO 80303, U.S.A.

ABSTRACT

Millimeter-wave propagation through the nonprecipitating atmosphere is modeled for frequencies below 1000 GHz. Complex refractivities represent the spectral properties of four natural absorbers; that is, oxygen, water-vapor, suspended droplets and ice particles. The *dry-air* model is supported by new, extensive 60-GHz laboratory absorption measurements of the pressure-broadened O_2 spectrum. The *water-vapor* model considers contributions of 30 local H_2O lines, which are supplemented by an empirical continuum term based on laboratory measurements in the 138- to 213-GHz range. Revised formulations for the complex permittivities of water and ice are employed in the *suspended-particle* model which, due to the Rayleigh approximation, provides only minimum estimates above 300 GHz.

1. INTRODUCTION

The natural atmospheric absorber of oxygen, water vapor, and suspended water or ice particles must be treated collectively in order to evaluate the effects of adverse weather on millimeter-wave system performance. A physical model is described here that predicts from meteorological variables the spectral characteristics of the absorbers up to 1000 GHz, taking into account recent advances in experimental and theoretical work. This paper presents formulations suitable for updates of the Near-Millimeter-Wave module of EOSAEL (Brown, 1987), as well as the analytical and numerical details.

In atmospheric radio-wave propagation the interaction of radiation with the medium is expressed by a complex refractivity, $N = N_o + N' + i\,N''$ ppm. The real part addresses changes in the propagation velocity (refraction) and the imaginary part quantifies the loss of radiation energy (absorption). The real part consists of a frequency-independent term, N_o, and of the dispersive refraction $N'(\nu)$. Both amplitude and phase response of a plane radio wave propagating a distance z at frequency ν through the atmosphere can be described by a complex field strength,

$$E(z) = \exp[\, i\,k\,z(\,1 + N\times10^{-6}\,)]\,E(0), \qquad (1)$$

where E(0) is the initial value, $k = 2\pi\nu/c$ is the free space wave number, and c is the speed of light in vacuum. For a homogeneous medium, refractivity N defines the path-specific quantities of power attenuation α and propagation delay τ as (frequency ν is in GHz throughout)

$$\alpha = 0.1820\,\nu\,N''(\nu)\ \text{dB/km} \quad \text{and} \quad \tau = 3.336\,[(N_o + N'(\nu)]\ \text{ps/km}. \qquad (2)$$

2. REFRACTIVITY SPECTRA OF THE GASEOUS ATMOSPHERE

2.1 MODELING SCHEME

Complex refractivity N is the key quantity computed by the Millimeter-wave Propagation Model "MPM" (Liebe, 1989). The practical N model consists of 44 O_2 and 30 H_2O local (centered below 1000 GHz) lines, of nonresonant spectra for dry air, and of an empirical water vapor continuum which reconciles experimental discrepancies. The model formulations for dry air and water vapor spectra follow closely the theory of absorption by atmospheric gases that is discussed in detail by Rosenkranz (1992). The Rayleigh absorption approximation is used for the refractivity of suspended water and ice particles (Liebe et al., 1989). The physical condition for a volume element of air is specified by

▪ barometric pressure	p	(0 to 1200	mb)
▪ ambient temperature	t	(- 100 to 50	°C)
▪ relative humidity	u	(0 to 100	%)
▪ suspended particle density	w	(0 to > 5	g/m^3).

For modeling purposes, a reciprocal temperature variable $\theta = 300/(t + 273.15)$ is introduced, and the total pressure, $p = p_d + e$ mb (1 mb = 100 Pa), is separated into partial pressures for dry air and water vapor. Water vapor pressure $e = (u/100)\, e_S$ is computed from the relative humidity u and the saturation pressure over water (-40 to 80°C) or ice (-100 to 0°C) at the temperature t by means of the Goff-Gratch (1946) formulations. Absolute humidity follows from $q = 0.7223\, e\, \theta$ g/m^3. An adequate approximations for saturation pressure over water is given by

$$e_S = 2.408\times10^{11}\, \theta^5 \exp(-22.644\, \theta) \;\; (\approx 35\times\theta^{-18}) \text{ mb.} \tag{3}$$

2.3 OXYGEN SPECTRUM

Refractivity by atmospheric oxygen is expressed by

$$N_D = N_1 + \Sigma_k S_k F_k + S_o F_o + i\, S_n F_n'' \text{ ppm,} \tag{4}$$

where the nondispersive term is given by $N_1 = 0.2588\, p_d\, \theta$ ppm, and line refractivity results from 44 O_2 resonances (k = line index). Each line strength,

$$S_k = a_1\, 10^{-6}\, p_d\, \theta^3 \exp[a_2 (1 - \theta)] \text{ kHz,} \tag{5}$$

is multiplied by the complex spectral shape function,

$$F(\nu) = \frac{\nu}{\nu_k} \left[\frac{1 - i\delta_k}{\nu_k - \nu - i\gamma_k} - \frac{1 + i\delta_k}{\nu_k + \nu + i\gamma_k} \right] \text{ GHz}^{-1}. \tag{6}$$

The Van Vleck-Weisskopf function $F(\nu)$ was modified by Rosenkranz (1988) to include line overlap effects. Width (γ) and overlap (δ) parameters of pressure-broadened O_2 lines in air are given by

$$\gamma_k = \{ [a_3\, 10^{-3} (p_d\, \theta^{0.8 - a4} + 1.10\, e\, \theta)]^2 + \gamma_Z^2 \}^{1/2} \text{ GHz} \tag{7}$$

$$\delta_k = (a_5 + a_6\, \theta) 10^{-3}\, p\, \theta^{0.8}. \tag{8}$$

Center frequencies ν_k and spectroscopic coefficients a_1 to a_6 are listed in Table 1. While only of interest below 10 mb (h ≥ 30 km), Zeeman-splitting of O_2 lines is approximated in Eq. (7) by a single linewidth, $\gamma_Z \approx 0.001$ GHz. A better approximation, $\gamma_Z \approx 25\,B_o$, takes into account the geomagnetic field B_o with values from (22 to 65)$\times 10^{-6}$ Tesla. Anisotropic effects due to the *anomalous Zeeman effect* of mesospheric O_2-lines have been detailed by Hufford and Liebe (1990).

Nonresonant refractivity arises below 10 GHz from the O_2 relaxation spectrum $S_o F_o$. Additionally, pressure-induced N_2 absorption $S_n F_n''$ makes a small contribution above 100 GHz. The associated strengths and shape factors are

$$S_o = 6.14\times 10^{-5}\, p_d\, \theta^2 \quad \text{and} \quad F_o(\nu) = -\nu\,(\nu + i\gamma_o)^{-1},$$
$$S_n = 1.40\times 10^{-12}\, p_d^2\, \theta^{3.5} \quad \text{and} \quad F_n''(\nu) \approx \nu\,(1.9\times 10^{-5}\,\nu^{1.5} + 1)^{-1}, \tag{9}$$

where the relaxation frequency is $\gamma_o = 0.56\times 10^{-3}\, p\, \theta^{0.8}$ GHz.

Absorption of dry air (e = 0) has been measured extensively in the laboratory (Liebe et al., 1990). Based on a best fit to these data (Liebe et al., 1992), the coefficients a_5 and a_6 have been revised. Further adjustments were made to the values for a_3 and $a_{5,6}$ listed in Table 1; that is, all γ_k were multiplied by 1.05 and all δ_k by 1.15. This correction reduced, on the average by 7 percent, the r.m.s. error of the residuals for all 5400 data points. An example of predicted attenuation rates and measured data points is depicted in Fig. 1.

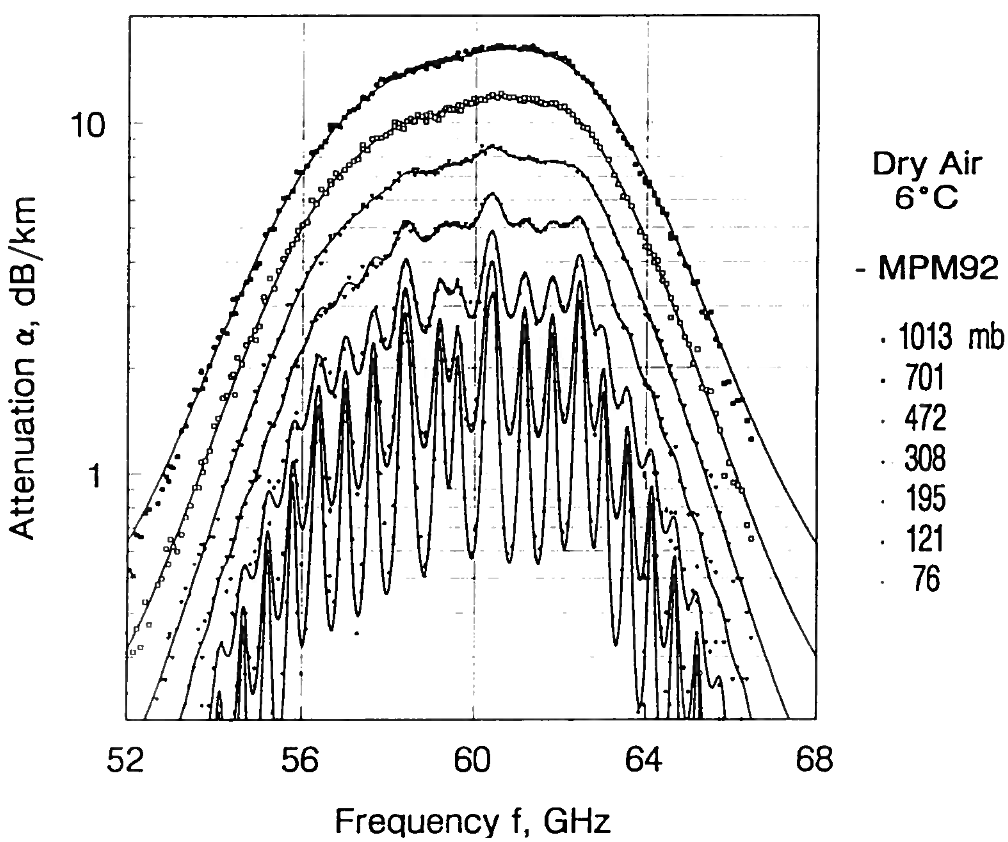

Figure 1. Dry air attenuation rates $\alpha(\nu)$ between 50 and 68 GHz at 6°C and pressures between 76 and 1013 mb: MPM predictions (solid lines) versus measured data (symbols).

TABLE 1. Spectroscopic Coefficients of O_2 Lines in Air

Line Center ν_k	Strength a_1	a_2	Width a_3	a_4	Overlap a_5	a_6
GHz	(kHz/mb)10^6		(GHz/mb)10^3		10^3 /mb	
50.474238	0.094	9.694	0.89	0	0.240	0.790
50.987749	0.25	8.694	0.91	0	0.220	0.780
51.503350	0.61	7.744	0.94	0	0.197	0.774
52.021410	1.41	6.844	0.97	0	0.166	0.764
52.542394	3.10	6.004	0.99	0	0.136	0.751
53.066907	6.41	5.224	1.02	0	0.131	0.714
53.595749	12.47	4.484	1.05	0	0.230	0.584
54.130000	22.80	3.814	1.07	0	0.335	0.431
54.671159	39.18	3.194	1.10	0	0.374	0.305
55.221367	63.16	2.624	1.13	0	0.258	0.339
55.783802	95.35	2.119	1.17	0	-0.166	0.705
56.264775	54.89	0.015	1.73	0	0.390	-0.113
56.363389	134.40	1.660	1.20	0	-0.297	0.753
56.968206	176.30	1.260	1.24	0	-0.416	0.742
57.612484	214.10	0.915	1.28	0	-0.613	0.697
58.323877	238.60	0.626	1.33	0	-0.205	0.051
58.446590	145.70	0.084	1.52	0	0.748	-0.146
59.164207	240.40	0.391	1.39	0	-0.722	0.266
59.590983	211.20	0.212	1.43	0	0.765	-0.090
60.306061	212.40	0.212	1.45	0	-0.705	0.081
60.434776	246.10	0.391	1.36	0	0.697	-0.324
61.150560	250.40	0.626	1.31	0	0.104	-0.067
61.800154	229.80	0.915	1.27	0	0.570	-0.761
62.411215	193.30	1.260	1.23	0	0.360	-0.777
62.486260	151.70	0.083	1.54	0	-0.498	0.097
62.997977	150.30	1.665	1.20	0	0.239	-0.768
63.568518	108.70	2.115	1.17	0	0.108	-0.706
64.127767	73.35	2.620	1.13	0	-0.311	-0.332
64.678903	46.35	3.195	1.10	0	-0.421	-0.298
65.224071	27.48	3.815	1.07	0	-0.375	-0.423
65.764772	15.30	4.485	1.05	0	-0.267	-0.575
66.302091	8.01	5.225	1.02	0	-0.168	-0.700
66.836830	3.95	6.005	0.99	0	-0.169	-0.735
67.369598	1.83	6.845	0.97	0	-0.200	-0.744
67.900867	0.80	7.745	0.94	0	-0.228	-0.753
68.431005	0.33	8.695	0.92	0	-0.240	-0.760
68.960311	0.13	9.695	0.90	0	-0.250	-0.765
118.750343	94.50	0.009	1.63	0	-0.036	0.009
368.498350	6.79	0.049	1.92	0.6	0	0
424.763124	63.80	0.044	1.93	0.6	0	0
487.249370	23.50	0.049	1.92	0.6	0	0
715.393150	9.96	0.145	1.81	0.6	0	0
773.839675	67.10	0.130	1.81	0.6	0	0
834.145330	18.00	0.147	1.81	0.6	0	0

2.4 WATER VAPOR SPECTRUM

Refractivity of atmospheric water vapor is represented by

$$N_V = N_2 + \sum_\ell S_\ell F_\ell + N_C \ \text{ppm}, \tag{10}$$

where nondispersive refractivity is given by $N_2 = (4.163\,\theta + 0.239)\, e\,\theta$ ppm, and line refractivity results from 30 local H_2O-resonances (ℓ = line index). The line strength,

$$S_\ell = b_1\, e\, \theta^{3.5} \exp\,[b_2\,(1 - \theta)] \ \text{kHz}, \tag{11}$$

is multiplied by the shape function, Eq. (6). The width of a pressure-broadened H_2O line follows the formulation given by Bauer et al. (1989),

$$\gamma_\ell = b_3\, 10^{-3} (p_d\, \theta^{b5} + b_4\, e\, \theta^{b6}) \ \text{GHz}. \tag{12}$$

Line overlap is neglected; i.e., $\delta_\ell = 0$. Table 2 lists for the center frequencies ν_ℓ the spectroscopic coefficients b_1 to b_6. Doppler-broadening of the lines is taken into account at pressures below 0.7 mb (h ≥ 60 km) by the approximation $\gamma_\ell^* = 0.535\,\gamma_\ell + (0.217\,\gamma_\ell^2 + \gamma_D^2)^{1/2}$, where the Doppler width is $\gamma_D = 1.46\times10^{-6}\, \nu_\ell\, \theta^{-1/2}$ GHz.

Continuum refractivity,

$$N_C = \nu\, e\, [0.998\, \nu\, (1 - 0.20\,\theta)\, \theta^{2.7} + i\,(0.357\, e\, \theta^{x} + 0.0113\, p_d\, \theta^{3.0})]\, 10^{-6} \ \text{ppm}, \tag{13}$$

addresses contributions to Eq. (10) that are in excess over the 30 local lines listed in Table 2. The real part is a first-order approximation to analytical results reported by Hill (1988). This part is small and insensitive to either a specific shape function or to dry-air pressure.

The imaginary part accounts empirically for absorption in excess of line contributions computed with the VanVleck-Weisskopf shape, Eq. (6). The strong negative temperature dependence of the e^2-term (exponent x) is still a source of controversy. Experimental and theoretical evidence for x are not in full agreement, as shown below:

ν, GHz	x(Exp.)	ν, GHz	x(Theory) [d]
137.8 [a]	10.5	30	6.5
190.3 [b]	8.4	120	6.7
213.5 [c]	7.5	360	10.2

[a] Liebe, 1889; [b] Bauer et al., 1991; [c] Godon et al., 1992; [d] Ma and Tipping, 1990.

Equation (13) is by and large supported by absolute absorption results from laboratory experiments on pure water vapor, and on mixtures with air [a] and nitrogen [b,c]. The current choice is x = 10.5; but an analysis is under way with the purpose of modifying Eq. (13), so that the reported evidence is more accurately reflected. The unusual temperature dependence has found a plausible interpretation by Ma and Tipping (1990). Their continuum theory relies only on far-wing contributions by the allowed rotational H_2O transitions (over 500 lines). Frequency and temperature are interwoven and the negative temperature dependence is predicted to become stronger as frequency increases.

TABLE 2. Spectroscopic Coefficients of H_2O Lines in Air

Line Center	Strength		Width			
ν_t	b_1	b_2	b_3	b_4	b_5	b_6
GHz	kHz/mb		(GHz/mb)10^3			
22.235080	0.0114	2.143	2.811	4.80	0.69	1.00
67.813960	0.00011	8.735	2.858	4.93	0.69	0.82
119.995940	0.00007	8.356	2.948	4.78	0.70	0.79
183.310074	0.230	0.668	2.813	5.30	0.64	0.85
321.225644	0.0046	6.181	2.303	4.69	0.67	0.54
325.152919	0.154	1.540	2.783	4.85	0.68	0.74
336.187000	0.0001	9.829	2.693	4.74	0.69	0.61
380.197372	1.1900	1.048	2.873	5.38	0.54	0.89
390.134508	0.0004	7.350	2.152	4.81	0.63	0.55
437.346667	0.0064	5.050	1.845	4.23	0.60	0.48
439.150812	0.0921	3.596	2.100	4.29	0.63	0.52
443.018295	0.0194	5.050	1.860	4.23	0.60	0.50
448.001075	1.060	1.405	2.632	4.84	0.66	0.67
470.888947	0.033	3.599	2.152	4.57	0.66	0.65
474.689127	0.128	2.381	2.355	4.65	0.65	0.64
488.491133	0.0253	2.853	2.602	5.04	0.69	0.72
503.568532	0.0037	6.733	1.612	3.98	0.61	0.43
504.482692	0.0013	6.733	1.612	4.01	0.61	0.45
556.936002	51.0	0.159	3.210	4.11	0.69	1.00
620.700807	0.509	2.200	2.438	4.68	0.71	0.68
658.006500	0.0274	7.820	3.210	4.14	0.69	1.00
752.033227	25.0	0.396	3.060	4.09	0.68	0.84
841.073593	0.0013	8.180	1.590	5.76	0.33	0.45
859.865000	0.0133	7.989	3.060	4.09	0.68	0.84
899.407000	0.0055	7.917	2.985	4.53	0.68	0.90
902.555000	0.0038	8.432	2.865	5.10	0.70	0.95
906.205524	0.0183	5.111	2.408	4.70	0.70	0.53
916.171582	0.856	1.442	2.670	4.78	0.70	0.78
970.315022	0.916	1.920	2.550	4.94	0.64	0.67
987.926764	13.8	0.258	2.985	4.55	0.68	0.90

Using a ground-based, zenith-viewing radiometer, Westwater et al. (1990) measured thermal emission at frequencies of 20.6, 31.7, and 90 GHz looking at identical air volumes. A radiosonde provided height profiles of p, t, and u. More than 100 data sets for clear air were converted to path attenuations and compared with MPM-predictions. Good agreement was obtained at 31.7 GHz and 90 GHz; whereas the 20.6-GHz data prompted us to raise the b_1 coefficient of the 22.2-GHz line by 5 percent.

Figure 2 displays the attenuation rate $\alpha(\nu)$ of moist air for a standard, sea-level condition. One notices more or less transparent window ranges (minimum absorption) centered around 35, 90, 140, 220 GHz. Measurement data reported by Furashov et al. (1988) for the 180- to 930-GHz range generally agree with MPM predictions.

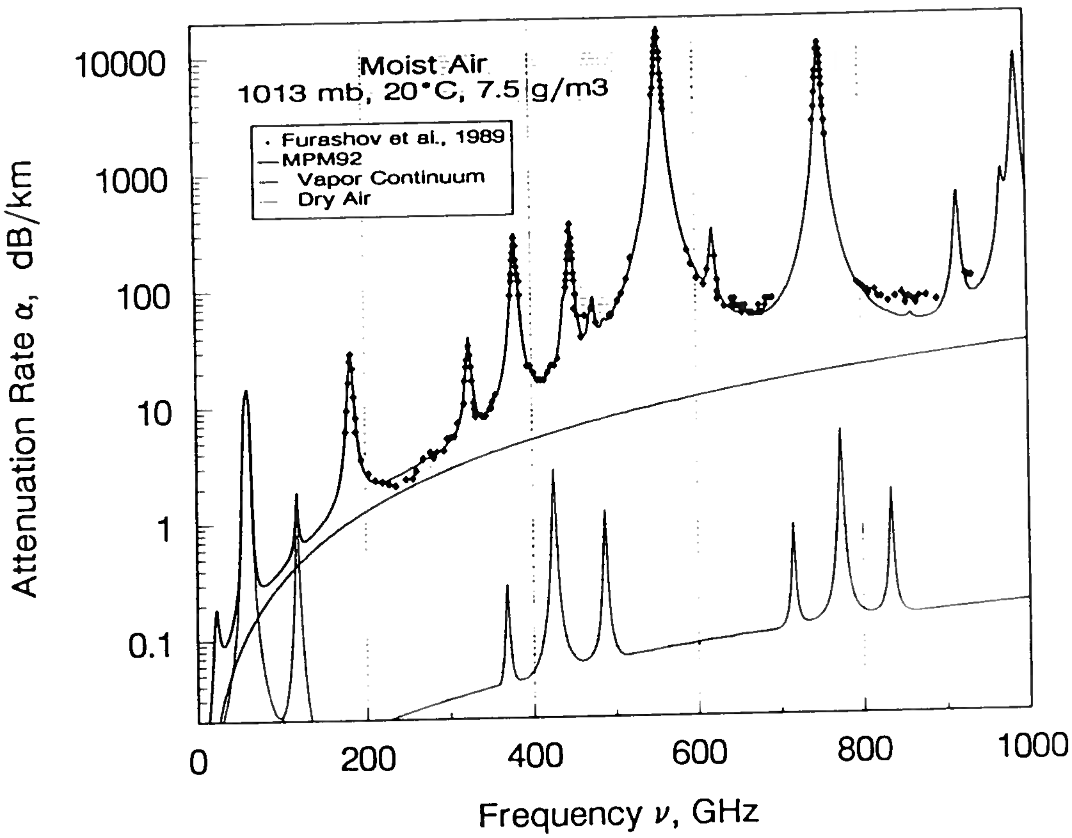

Figure 2. Predicted attenuation rate α of moist ($q = 7.5$ g/m^3) and dry air up to 1000 GHz for a standard sea-level condition.

---

3. SUSPENDED WATER/ICE PARTICLE SPECTRA

3.1 RAYLEIGH APPROXIMATION

The interaction of suspended water droplets and ice particles with radio waves is treated with the Rayleigh absorption approximation ($c/\nu \gg 2r$),

$$N_{w,i} = 1.5\,(w / m_{w,i})[(\epsilon_{w,i} - 1) / (\epsilon_{w,i} + 2)], \tag{14}$$

where $m_{w,i}$ = 1.000 and 0.916 (g/cm^3) are specific weights, and $\epsilon_{w,i}$ are complex permittivities of water and ice, respectively (Liebe et al., 1989). For the size spectra (radii $r \leq 50$ μm) of suspended water droplets, Eq. (14) is valid up to 300 GHz and, disregarding scattering, provides minimum estimates up to 1000 GHz. Fog or cloud conditions are modeled with the mass density of suspended particles, w (0 to ≥ 5 g/m^3). Above freezing ($t \geq 0$°C), water droplets form when the relative humidity exceeds saturation slightly; that is, u = 100 to 101 %.

3.2 COMPLEX PERMITTIVITY OF WATER AND ICE

Complex permittivity of Water may be approximated by a double-Debye model (Liebe et al., 1991),

$$\epsilon_w = \epsilon_o - \nu\,[(\epsilon_o - \epsilon_1) / (\nu + i\,\gamma_1) + (\epsilon_1 - \epsilon_2) / (\nu + i\,\gamma_2)], \tag{15}$$

which realizes a best fit to measured values with the following coefficients:

Static (ν = 0) permittivity	$\epsilon_o = 77.66 + 103.3\,(\theta - 1)$,	
high-frequency permittivities	$\epsilon_1 = 0.0671\,\epsilon_o$,	$\epsilon_2 = 3.52$;
relaxation frequencies	$\gamma_1 = 20.20 - 146\,(\theta - 1) + 316\,(\theta - 1)^2$,	$\gamma_2 = 39.8\,\gamma_1$ GHz.

The temperature dependence of ϵ_2 was eliminated to avoid for super-cooled (-20 to -40°C) water nonphysical behavior at frequencies above 100 GHz.

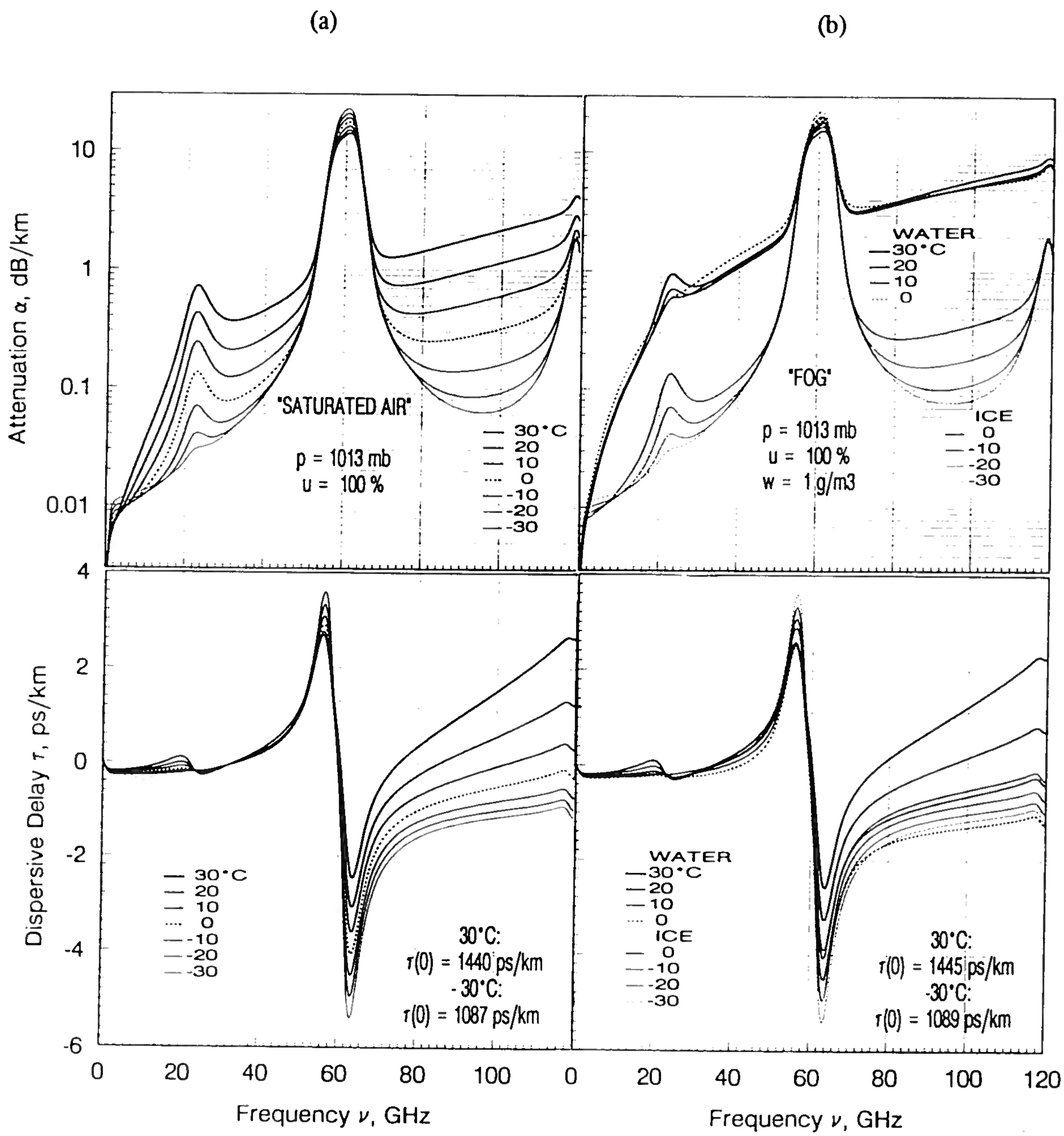

Figure 3. Attenuation and Delay Spectra between 0 and 120 GHz at Temperatures ±30°C: (a) Saturated Air at Sea-Level, u = 100 %, (b) Water and Ice Fog, w = 1 g/m^3.

Figure 3 gives examples of predicted attenuation and delay spectra for saturated, sea-level air with a normalized density of $w = 1$ g/m^3 (heavy fog, about 50 m visibility). One notices that from 1 to 100 GHz the overall attenuation behavior is between 0 and 30°C almost independent of temperature. The refractive delay is given by $\tau(0) = 3.336\,(N_1 + N_2 + N_3)$, where $N_3 = 1.5\,w\,[1 - 3/(\epsilon_o - 1)]$.

A permittivity model for ICE was reported by Hufford (1991),

$$\epsilon_i = 3.15 + i\,(a_i/\nu + b_i\,\nu), \tag{16}$$

where $a_i(\theta) = (\theta - 0.171)\exp(17.0 - 22.1\,\theta)$ GHz, and
$b_i(\theta) = \{0.0542\,[\theta/(\theta - 0.993)]^2 + (6.33/\theta) - 1.31\}10^{-5}$ GHz^{-1}.

Equation (16) is valid for $t \leq 0$°C ($\theta \geq 1.099$) over the frequency range from 1 MHz to 1000 GHz. Propagation effects caused by suspended ice crystals (needles and plates) are primarily depolarizing in nature. Ice attenuation and delay rates (see Fig. 3) were estimated with Eq. (14).

5. SUMMARY

Systems that operate at millimeter-wave frequencies offer much improved performance over infrared/optical systems under fog or cloud conditions. Propagation characteristics of the nonprecipitating atmosphere are predicted by the refractivity model, $N = N_D + N_V + N_{W,I}$ [Eqs. (4), (10), (14)]. Transmission and emission properties of the inhomogeneous atmosphere (e.g., opacity, path delay, brightness temperature) can be modeled when the path distributions of pressure, temperature, and humidity are known. The suspended particle density w might be estimated from databases for the extinction of visible light.

Uncertainties of MPM predictions may be evaluated by comparison with data for which the true values of p, t, u, and w are known. However, such measurements cannot be made reliably under "real" atmospheric conditions. Under "controlled" laboratory conditions, the dry-air absorption has been measured between 49 and 67 GHz. The extensive experimental data set agrees with MPM predictions to within 1 percent (Liebe et al., 1992). The errors of model predictions involving H_2O vapor and water droplets are estimated to lie in the 10 percent range. Validation and error checking of predictions, as well as incorporating new research results into MPM, will continue to be critical and time-consuming tasks.

ACKNOWLEDGMENT

This work was supported in part by the U. S. Army Atmospheric Sciences Laboratory, ARL, SLCAS-BA under Reference No. ASL 92-8058.

REFERENCES

Bauer, A., M. Godon, M. Kheddar, and J. M. Hartmann, 1989: Temperature and Perturber Dependences of Water Vapor Line-Broadening: Experiments at 183 GHz, Calculations Below 1000 GHz. J. Quant. Spectr. Radiat. Transf., 41(1):49-54.

Bauer, A., and M. Godon, 1991: Temperature Dependence of Water Vapour Absorption in Line-wings at 190 GHz. J. Quant. Spectr. Rad. Transf., 46(3):211-220.

Brown, D. R., 1987: Near Millimeter Wave Module, NMMW, ASL-TR-0221-6, U.S. Army Atmosperic Sciences Laboratory, White Sands Missile Range, NM 88002-5501.

Furashov, N. I., V. Yu. Katkov, and B. A. Svertlov, 1989: Submillimetre Spectrum of the Atmospheric Water Vapor Absorption - Some Experimental Results. ICAP 89, IEE Conf. Publ., No. 301:310-311.

Godon, M., J. Carlier, and A. Bauer, 1992: Laboratory Studies of Water Vapor Absorption in the Atmospheric Window at 213 GHz. J. Quant. Spectr. Radiat. Transf., 47(4):275-285.

Goff, J. A., and S. Gratch, 1946: Low-Pressure Properties of Water from -160 to 212°F. Trans. Amer. Soc. Heat. Vent. Eng., 52:95-121 (also List, R. J., Smithonian Meteorological Tables. Washington D.C., Smithonian Inst., Sixth Ed., 1966).

Hill, R. J., 1988: Dispersion by Atmospheric Water Vapor at Frequencies Less Than 1 THz. IEEE Trans. Antennas Propag., AP-36(3):423-430.

Hufford G. A., and H. J. Liebe, 1989: Millimeter-Wave Propagation In The Mesosphere. NTIA-Report 89-249, U.S. Dept. Com., Boulder, CO; NTIS Order No. PB 90-119868/AF (1989).

Hufford, G. A., 1991: A Model for the Complex Permittivity of Ice at Frequencies Below 1 THz. Int. J. Infrared and Millimeter Waves, 12(7): 677-680.

Liebe, H. J., 1989: MPM - An Atmospheric Millimeter-Wave Propagation Model. Int. J. Infrared and Millimeter Waves, 10(6): 631-650.

Liebe, H. J., T. Manabe, and G. A. Hufford, 1989: Millimeter-Wave Attenuation and Delay Rates Due to Fog/Cloud Conditions. IEEE Trans. Antennas Propag., AP-37(12):1617-1623.

Liebe, H. J., G. A. Hufford, and T. Manabe, 1991: A Model for the Complex Permittivity of Water at Frequencies Below 1 THz. Int. J. Infrared and Millimeter Waves, 12(7):659-675.

Liebe, H. J., P. W. Rosenkranz, and G. A. Hufford, 1992: Atmospheric 60-GHz Oxygen Spectrum: New Measurements and Line Parameters. J. Quant. Spectr. Radiat. Transf., 48(5): in press.

Ma, Q., and R. H. Tipping, 1990: Water Vapor Continuum in the Millimeter Spectral Region. J. Chem. Phys., 93(9):6127-6139.

Rosenkranz, P. W., 1988: Interference Coefficients for Overlapping Oxygen Lines in Air. J. Quant. Spectr. Radiat. Transf., 39(4):287-297.

Rosenkranz, P. W., 1992: Absorption of Microwaves by Atmospheric Gases. In Atmospheric Remote Sensing By Microwave Radiometry, Chap. 2; M. A. Janssen, ed., Wiley and Sons, N.Y., N.Y. (in press).

Westwater, Ed. R., J. B. Snider, and M. J. Falls, 1990: Ground-Based Radiometric Observations of Atmospheric Emission and Attenuation at 20.6, 31.65, and 90.0 GHz: A Comparison of Measurements and Theory. IEEE Trans. Antennas Propag., AP-38(10):1569-1580.